Inverse Kinematics Proton Scattering on ^{18}Ne and Mirror Symmetry in $A = 18$ Nuclei

L. A. Riley,[1,*] J. K. Jewell,[1,†] P. D. Cottle,[1] T. Glasmacher,[2,3] K. W. Kemper,[1] N. Alamanos,[4] Y. Blumenfeld,[5] J. A. Carr,[6] M. J. Chromik,[2] R. W. Ibbotson,[2] F. Maréchal,[5] W. E. Ormand,[7] F. Petrovich,[1] H. Scheit,[2] and T. Suomijärvi[5]

[1]*Department of Physics, Florida State University, Tallahassee, Florida 32306-4350*
[2]*National Superconducting Cyclotron Laboratory, Michigan State University, East Lansing, Michigan 48824*
[3]*Department of Physics and Astronomy, Michigan State University, East Lansing, Michigan 48824*
[4]*CEA/DSM/DAPNIA/SPhN Saclay, F-91191 Gif sur Yvette Cedex, France*
[5]*Institut de Physique Nucléaire, IN2P3-CNRS, F-91406 Orsay, France*
[6]*Supercomputer Computations Research Institute, Florida State University, Tallahassee, Florida 32306*
[7]*Department of Physics and Astronomy, Louisiana State University, Baton Rouge, Louisiana 70803-4001*

(Received 18 December 1998)

The $0^+_{\text{g.s.}} \rightarrow 2^+_1$ transition in ^{18}Ne has been studied using the inverse kinematics reaction $p(^{18}\text{Ne}, p')$ with a radioactive ^{18}Ne beam at 30 MeV/nucleon. Hadronic scattering data on the $0^+_{\text{g.s.}} \rightarrow 2^+_1$ transition in the mirror nucleus ^{18}O are already available, so this is the first time that hadronic measurements have been available to test mirror symmetry in *s-d* shell nuclei. The angular distribution data for proton inelastic scattering in ^{18}Ne and corresponding data for ^{18}O are well reproduced in microscopic model calculations using empirical proton and neutron transition densities determined for ^{18}O. [S0031-9007(99)09179-6]

PACS numbers: 21.10.–k, 25.40.Ep, 25.60.–t, 27.20.+n

Since the time of Rutherford, nearly ninety years ago, the static and dynamic properties of the nucleus have been studied using a wide array of experimental probes [1]. With the advent of new radioactive beam facilities [2], it is now possible to extend these studies to unstable nuclei. In this Letter, we report new inelastic proton scattering data for the $0^+_{\text{g.s.}} \rightarrow 2^+_1$ transition in ^{18}Ne obtained via the scattering of a radioactive ^{18}Ne beam from a proton target. This is the heaviest $Z > N$ nucleus for which proton scattering data have been reported. These data provide the first hadronic test of mirror symmetry [3] for quadrupole transitions in *s-d* shell nuclei. The $0^+_{\text{g.s.}} \rightarrow 2^+_1$ transition in ^{18}O has been studied earlier via scattering of nucleons [4–6], pions [7], and electrons [8]. Previously, the only type of data available on this transition in both ^{18}O and ^{18}Ne was from the $2^+_1 \rightarrow 0^+_{\text{g.s.}}$ γ-ray decay [9]. The γ-decay data are sensitive only to proton transition densities, while hadronic data are sensitive to both proton and neutron densities [1,10]. Here we describe the present measurement of proton scattering on ^{18}Ne and compare data from inelastic scattering of low energy nucleons on both ^{18}O and ^{18}Ne to consistent folding model calculations using empirical densities obtained for ^{18}O.

We measured angular distributions for protons scattered from the ground and 1.89 MeV 2^+_1 states of ^{18}Ne by the $p(^{18}\text{Ne}, p')$ reaction. The 30 MeV/nucleon ^{18}Ne beam was produced in the A1200 fragment separator [11] at the National Superconducting Cyclotron Laboratory via fragmentation of a 65 MeV/nucleon ^{20}Ne primary beam on a water cooled 360 mg/cm^2 ^{9}Be target. A 200 mg/cm^2 ^{12}C achromatic degrading wedge subtending an angle of 1.9 mrad and placed at the second dispersive image of the A1200 was used to reduce the number of beam species transmitted, and the momentum acceptance of the A1200 was 1%. The secondary beam was approximately 90% pure. The main contaminant was ^{17}F, which accounted for about 7% of the beam intensity. Beam particles were stopped in a fast/slow plastic phoswich telescope which allowed clear separation of the ^{18}Ne from ^{17}F and other beam contaminants on an event-by-event basis. The intensity of the beam at the target position—as measured in the phoswich telescope—reached a maximum of 30 000 particles/sec and averaged 25 000 particles/sec during the experiment. Approximately 25% of the beam particles which exited the A1200 reached the target.

Polypropylene foils were used as the hydrogen targets for the secondary beam. At different times during the experiment, foils of different thicknesses (1.1 and 3.6 mg/cm^2) were used, but it was found that both thicknesses yielded high quality data. The foils were mounted at 55° with respect to the beam axis to minimize the angular straggling of scattered protons leaving the target. The beam was tracked on a particle-by-particle basis by two position sensitive parallel plate avalanche counters [12] upstream of the target chamber. Data were also taken with a 3 mg/cm^2 ^{12}C target in order to evaluate the background caused by the carbon in the polypropylene.

The arrangement for detecting the scattered protons was quite similar to that used by Kelley *et al.* for a measurement of the $p(^{38}\text{S}, p')$ reaction [13]. Scattered protons were detected using the FSU-MSU array of Si strip-Si PIN-CsI particle telescopes. The telescopes have an active area of 5 cm × 5 cm and were mounted 28 cm from the target position, yielding a total laboratory-frame

 0031-9007/99/82(21)/4196(4)$15.00

field of view of 10° for each telescope. The 300-μm-thick strip detectors consisted of 16 3-mm-wide strips. The 470 μm PIN diode and 1 cm CsI layers stopped higher energy protons. Protons stopped in the strip detectors were identified by time-of-flight, while higher energy protons were identified in gates on the ΔE-E spectra. The telescopes were oriented such that the Si strips were tangent to circles of constant scattering angle with respect to the beam line alignment axis. Because of finite strip width and the fact that the strips were not curved to follow lines of constant scattering angle, the geometric field of view of each strip, corresponding to an uncertainty in scattering angle measurements, was approximately 0.85°.

Three telescopes were mounted with their centers at laboratory-frame angles of 75° and three were centered at 70°. Hence, we detected protons in the laboratory scattering angle range 65°–80°, corresponding to a center-of-mass angular range of approximately 20°–45°. The laboratory energy range of detected protons was 1–22 MeV, sufficient to detect protons which were elastically scattered and inelastically scattered to the 2_1^+ state in the detected angular range.

The scattered proton data are presented in the form of a lab-frame kinetic energy vs scattering angle spectrum and compared to calculated kinematics curves in Fig. 1. The data shown are in coincidence with both beam and proton identification gates. Scattering angles have been determined from Si strip positions and beam tracking information. Clear separation between elastic and inelastic events was obtained. The absence of a significant background is also apparent. In total, 10 400 elastically scattered and 112 inelastically scattered protons were collected during the 38 hour experiment. The data taken with the ^{18}Ne on the ^{12}C target yielded no evidence of any contributions to the proton data from the carbon in the polypropylene target.

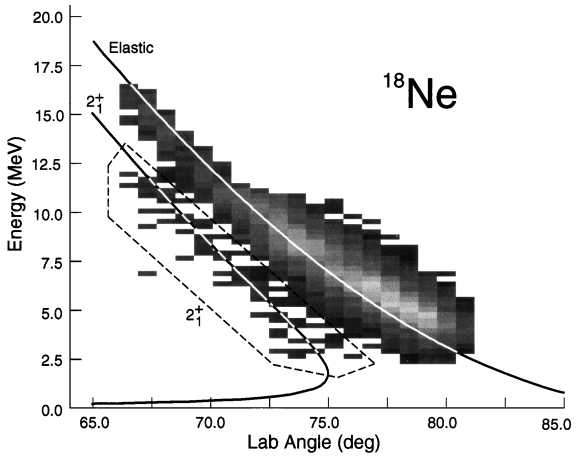

FIG. 1. Proton laboratory energy vs scattering angle for the data from $p(^{18}\mathrm{Ne}, p')$. The solid curves show the calculated kinematics for comparison.

The natural binning of the data by the Si strips in the laboratory was used to generate the proton angular distributions. It should be noted that this leads to a difference in scattering angles for elastic and inelastic points in the center of mass for each bin. The inelastic points have been generated using two strips each due to lower yields. To provide absolute normalizations—and thus absolute differential cross sections—the elastic scattering data were compared to an angular distribution calculated using optical model parameters from the 30 MeV $^{20}\mathrm{Ne}(p, p')$ study of de Swiniarski *et al.* [14]. The elastic scattering data were normalized on a telescope-by-telescope basis, so that the relative cross sections obtained from each strip in the same telescope were not altered.

If the nuclei ^{18}O and ^{18}Ne are mirror symmetric, then the proton ground state and transition densities in ^{18}O should be equal to the corresponding neutron densities in ^{18}Ne, while the neutron densities in ^{18}O and proton densities in ^{18}Ne should be equal as well, to the extent that Coulomb effects are small [3]. Below we describe folding model calculations to test this hypothesis. Proton densities (ρ_p) for the ground state and $0^+_{\mathrm{g.s.}} \rightarrow 2^+_1$ transition in ^{18}O have been determined from electron scattering [8]. A study of ^{18}O via the scattering of 135 MeV protons provided corresponding information on neutron densities (ρ_n) in this nucleus [6]. The neutron and proton multipole matrix elements for the empirical quadrupole densities are $M_n = 6.18$ fm^2 and $M_p = 3.00$ fm^2, with $M_n/M_p = 2.06$ in the convention in which $B(E2; 0^+_{\mathrm{g.s.}} \rightarrow 2^+_1) = 5M_p^2$.

Our current theoretical knowledge of effective interactions for nucleon-nucleus scattering is very solid [1]; however, the most extensive empirical work has been done for incident nucleon energies in excess of 100 MeV [15]. At the lower energy of interest here, empirical studies have been largely restricted to elastic scattering [16]. In one comprehensive study, an excellent description of available 25–50 MeV nucleon scattering data from ^{6,7}Li has been obtained using a consistent theoretical microscopic single scattering model [17] employing a realistic effective interaction adopted from the work of Mahaux and collaborators [18,19] and Bertsch *et al.* [20]. An important feature of the nucleon-nucleus effective interaction in this energy region is that $v_{pn} \approx v_{np} \approx 3v_{pp} \approx 3v_{nn}$ [1,10]. Much of the available angular distribution data on elastic and $L = 2$ inelastic scattering on ^{6,7}Li at these energies were reproduced with high precision (better than 15%) over large angular ranges. Two exceptions to this success should be noted. First, the ^{6,7}Li calculations were less successful at large angles ($\theta_{\mathrm{c.m.}} > 60°$) where coupled channels and core exchange effects—both neglected in those calculations—become important. Second, the authors of Ref. [17] noted inconsistencies among the data sets they analyzed so that some of the angular distribution results are reproduced with much higher accuracy than others.

Here the model of Ref. [17] is applied to the present 30 MeV ^{18}Ne(p, p') data using the empirical ^{18}O densities obtained from electron scattering [8] and intermediate energy proton scattering [6] analyses. As in Ref. [17], the present calculations were performed with the computer codes ALLWRLD [21] and TAMURA [22]. The ρ_p in ^{18}Ne are taken to be equal to the ρ_n determined for ^{18}O via proton scattering, and the ρ_n for ^{18}Ne are set equal to the ρ_p in ^{18}O determined from electron scattering. Additional results for ^{18}O(n, n') at $E_n = 24.0$ MeV [5] and ^{18}O(p, p') at $E_p = 24.5$ MeV [4] are also presented for comparison. The reaction ^{18}O(n, n') is the mirror reaction to ^{18}Ne(p, p').

As can be seen in the theoretical results shown in Fig. 2, the calculations reproduce the experimental data extremely well, particularly for $\theta_{\text{c.m.}} < 60°$, which is quite impressive considering that there are no free parameters and extensive tuning of the nucleon-nucleus interaction has yet to be carried out in this energy region. The case for mirror symmetry is well supported by these results. The precision of the present test for mirror symmetry is limited by both the reaction model and the quality of the ^{18}Ne inelastic scattering data: a violation of mirror symmetry could be seen if the differential cross sections deviated by more than 30% from the predicted magnitudes.

Also shown as dashed curves in Fig. 2 are results obtained assuming $M_n/M_p = N/Z$ for the $0^+_{\text{g.s.}} \rightarrow 2^+_1$ transitions in mass 18 with ρ_n in ^{18}Ne and ρ_p in ^{18}O taken from electron scattering on ^{18}O [8]. The empirical densities have $M_p/M_n > Z/N$ for ^{18}Ne and $M_n/M_p > N/Z$ for ^{18}O. The dashed curves clearly underestimate the experimental data in all cases. The differences between the dashed and solid curves are nearly identical for the ^{18}Ne(p, p') and ^{18}O(n, n') mirror reactions. A larger difference is obtained in the case of ^{18}O(p, p') because in ^{18}Ne(p, p') and ^{18}O(n, n') the coupling between the projectile and underestimated target density is only about one-third of that for ^{18}O(p, p'), as noted above.

The result $M_p/M_n > Z/N$ is expected for low-lying quadrupole transitions in a closed neutron shell nucleus like ^{18}Ne. In the extreme shell model only the valence protons would contribute to the transition and M_p/M_n would be infinite. Even with configuration mixing in the proton valence space M_p/M_n remains infinite. Mixing with complicated near space configurations, i.e., deformed states [23,24], and core polarization, i.e., coupling to giant resonances [25–27], drives M_p/M_n toward Z/N. However, Z/N tends not to be achieved in single closed shell nuclei [28].

In summary, we have measured the angular distributions for ^{18}Ne + p elastic and $0^+_{\text{g.s.}} \rightarrow 2^+_1$ inelastic scattering using the inverse kinematics reaction $p(^{18}\text{Ne}, p')$ with a radioactive ^{18}Ne beam at 30 MeV/nucleon. The measured angular distribution for the inelastic scattering to the 2^+_1 state of ^{18}Ne is well reproduced using proton and neutron transition densities which are "mirrors" of empirical transition densities for ^{18}O. That is, mirror symmetry is qualitatively satisfied for the $0^+_{\text{g.s.}} \rightarrow 2^+_1$ transitions in ^{18}Ne and ^{18}O to the precision of the present experiment and theory. Altogether, we have demonstrated the utility of recent advances in radioactive beam technology for expanding our understanding of the dynamical properties of nuclei outside the valley of stability. Although the theoretical cross section results that have been presented are good, it is clear that additional work must be done to gain a greater understanding of the components of the microscopic single scattering model for nucleon-nucleus scattering at energies below 100 MeV if these unstable nuclei are to be studied in even greater detail.

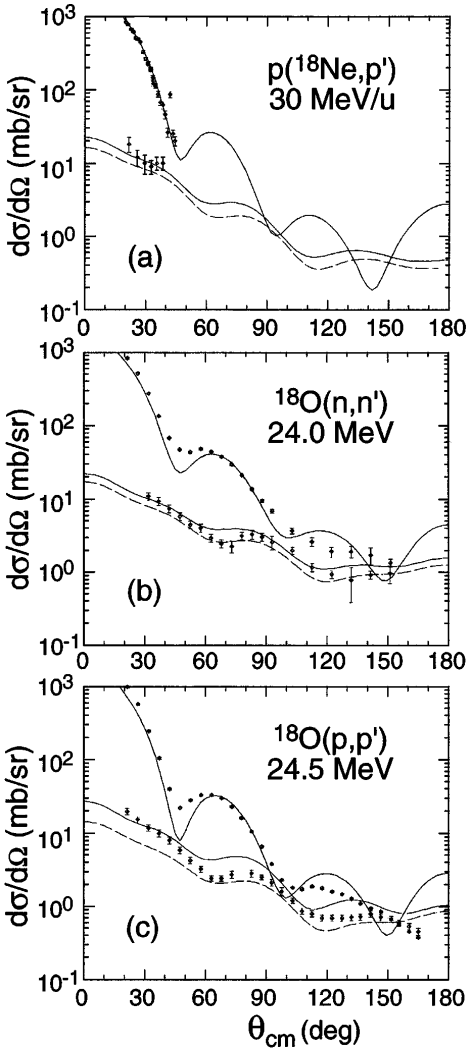

FIG. 2. Comparison of data for the $0^+_{\text{g.s.}} \rightarrow 2^+_1$ transition from (a) the present $p(^{18}\text{Ne}, p')$ reaction, (b) ^{18}O(n, n') reaction at 24.0 MeV [5], and (c) the ^{18}O(p, p') reaction at 24.5 MeV [4] to microscopic scattering calculations based on empirical densities for both protons and neutrons (solid curves) and densities set to obey the relationship $M_n/M_p = N/Z$ (dashed curves). The calculations are described in detail in the text.

This work was supported by the National Science Foundation through Grants No. PHY-9523974, No. PHY-9528844, and No. PHY-9602927.

*Present address: Department of Physics and Astronomy, Earlham College, Richmond, IN 47374.
†Present address: Idaho National Engineering Laboratory, Idaho Falls, ID 83415.

[1] F. Petrovich, J. A. Carr, and H. McManus, Annu. Rev. Nucl. Part. Sci. **36**, 29 (1986).
[2] P. G. Hansen, Nucl. Phys. **A630**, 285 (1998).
[3] A. M. Bernstein, V. R. Brown, and V. A. Madsen, Phys. Rev. Lett. **42**, 425 (1979).
[4] J. L. Escudie *et al.*, Phys. Rev. C **10**, 1645 (1974).
[5] P. Grabmayr, J. Rapaport, and R. W. Finlay, Nucl. Phys. **A350**, 167 (1980).
[6] J. Kelly *et al.*, Phys. Lett. **169B**, 157 (1986).
[7] S. Iversen *et al.*, Phys. Rev. Lett. **40**, 17 (1978); S. Iversen, Ph.D. thesis, Northwestern University (Los Alamos Technical Report LA-7828, 1979).
[8] B. E. Norum *et al.*, Phys. Rev. C **25**, 1778 (1982).
[9] S. Raman *et al.*, At. Data Nucl. Data Tables **36**, 1 (1987).
[10] A. M. Bernstein, V. R. Brown, and V. A. Madsen, Phys. Lett. **103B**, 255 (1981).
[11] B. M. Sherrill *et al.*, Nucl. Instrum. Methods Phys. Res., Sect. B **56**/**57**, 1106 (1991).
[12] D. Swan, J. Yurkon, and D. J. Morrissey, Nucl. Instrum. Methods Phys. Res., Sect. A **348**, 314 (1994).
[13] J. H. Kelley *et al.*, Phys. Rev. C **56**, R1206 (1997).
[14] R. de Swiniarski *et al.*, Can. J. Phys. **52**, 2422 (1974).
[15] J. J. Kelly, Phys. Rev. C **39**, 2120 (1989).
[16] J. S. Petler, M. S. Islam, R. W. Finlay, and F. S. Dietrich, Phys. Rev. C **32**, 673 (1985).
[17] F. Petrovich *et al.*, Nucl. Phys. **A563**, 387 (1993).
[18] J. P. Jeukenne, A. Lejeune, and C. Mahaux, Phys. Rev. C **10**, 1391 (1974); Phys. Rep. **25C**, 83 (1976); Phys. Rev. C **15**, 10 (1977).
[19] J. P. Jeukenne, A. Lejeune, and C. Mahaux, Phys. Rev. C **16**, 80 (1977).
[20] G. Bertsch *et al.*, Nucl. Phys. **A284**, 399 (1977).
[21] J. A. Carr *et al.* modification of 1985 version of the computer program ALLWRLD (unpublished).
[22] J. A. Carr *et al.* 1985 version of the computer program TAMURA (unpublished); T. Tamura, W. R. Coker, and F. Rybicki, Comput. Phys. Commun. **2**, 94 (1971).
[23] B. A. Brown, A. Arima, and J. B. McGrory, Nucl. Phys. **A277**, 77 (1977).
[24] E. K. Warburton, B. A. Brown, and D. J. Millener, Phys. Lett. B **293**, 7 (1992).
[25] S. Siegel and L. Zamick, Nucl. Phys. **A145**, 89 (1970).
[26] V. R. Brown and V. A. Madsen, Phys. Rev. C **11**, 1298 (1975).
[27] F. Petrovich *et al.*, Phys. Rev. C **16**, 839 (1977).
[28] V. A. Madsen and V. R. Brown, Phys. Rev. Lett. **52**, 176 (1984).